Multiple diffraction of X-Rays in many-crystal systems

Victor Kohn

Russian Research Centre "Kurchatov Institute", 123182 Moscow, Russia

date: June, 1998; file: hl-muld2.ps

The document is the part of Hamburg lectures
"Selected topics in the theory of coherent scattering of X-rays"

Contents:

1. INTRODUCTION

The theoretical investigation of the multiple diffraction of X-Ray plane waves in one crystal plate is of interest from the fundamental point of view. However, from a practical point of view the many-crystal systems are always of interest. First of all, it is so because the plane wave does not exist in nature. Secondly, for managing different devices like monochromators, collimator or reflectors usually one crystal plate is not enough. The experimental setup in which the phenomenon of multiple diffraction is studied, naturally, may demand to use the same multiple diffraction case for collimating the incident beam. If the multiple diffraction occurs in several independent crystals then the calculation must be performed successively in each crystal taking into account that the properties of the beam may be changed by preceding crystals. There are two different simple experimental arrangements which realize the many-crystal system.

First one deals with the different blocks of the same crystal cut out on the same basis but having different orientation of boundaries in different blocks which are divided in space. The example of such a system is shown in Fig.1 (left). Usually in this case a coplanar diffraction (energy dependent) is convenient. The blocks have completely the same crystal lattice but independent boundaries.

The second setup consists of the multilayer crystal system where the neighboring layers have the boundaries in common and all boundaries are parallel to each other.

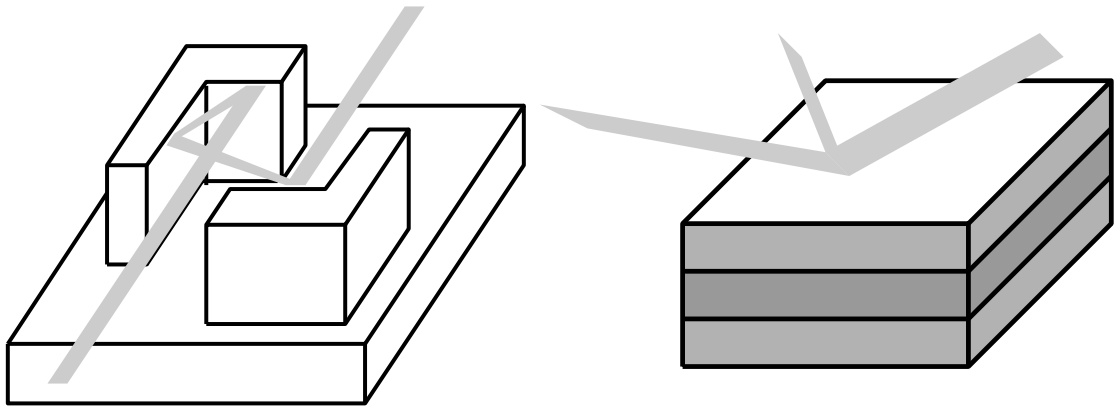

FIG. 1. Monochromator of three-beam coplanar diffraction (left) and three-beam diffraction in multilayer crystal systems (right)

However, the crystal lattice parameters may be different in different layers. When the crystal lattice parameters differ only slightly the multiple diffraction occurs in each layer but under slightly different conditions. However, in some layers where the crystal lattice parameters differ strongly the multiple diffraction is absent, however, many beams travel through these layers if these are inside the multilayer system. Such a device is shown schematically in Fig.1 (right).

In this topic we consider the equations which are necessary for calculating the system pointed above in addition to the calculating scheme for one crystal plate considered in a separate topic. The case of coplanar diffraction is accompanied a series of examples where the results of calculation of properties of specific possible systems are presented. The case of multilayer system is developed weakly up to now, so it is future science. Therefore only the equations are presented here.

2. COPLANAR MULTIPLE DIFFRACTION DEVICES. GENERAL THEORY.

The device of the first kind is of practical interest in the case of coplanar diffraction when all the beams lie at the same plane and this plane may be parallel to the basis of the device. The interferometer or the monochromator can be considered. In a cubic crystal like Silicon the critical wavelength λ_c of coplanar three-beam diffraction on the reciprocal lattice vectors $\mathbf{h}_1$ and $\mathbf{h}_2$ having the indexes h_1, k_1, l_1 and h_2, k_2, l_2, is defined by the relation

$$\lambda_c = \frac{4\pi \sin\varphi}{|\mathbf{h}_1 - \mathbf{h}_2|} = 2a\sqrt{\frac{1-A}{B}} \tag{1}$$

where φ is an angle between the vectors $\mathbf{h}_1$ and $\mathbf{h}_2$, and

$$A = \frac{(h_1h_2 + k_1k_2 + l_1l_2)^2}{(h_1^2 + k_1^2 + l_1^2)(h_2^2 + k_2^2 + l_2^2)}, \qquad B = (h_1 - h_2)^2 + (k_1 - k_2)^2 + (l_1 - l_2)^2 \tag{2}$$

For example, in the three-beam case on (440) and (044) reflections in the Silicon crystal ($a = 5.43$ Å) the critical wavelength $\lambda_c = 2\pi/K_c = 1.663$ Å that is very close to the Ni K_α fluorescent radiation of X-ray tube. In the case involving (880) and (488) reciprocal lattice vectors $\lambda_c = 2\pi/K_c = 0.859$ Å, that is very close to the ^{57}Fe nuclear resonance ($\lambda = 0.860$ Å).

In the coplanar case the polarization vectors $\mathbf{e}_m^\pi$, as chosen according to Fig. 6 of the topic describing the diffraction in one crystal (we will call it later as topic I.), are equal to each other and normal to the scattering plane which is a plane of vectors $\mathbf{s}_m$ and $\mathbf{e}_m^\sigma = [\mathbf{s}_m \times \mathbf{e}_m^\pi]$, $m = 0, 1, 2$. In the approximation when only the E1-transition (electric dipole interaction) is taken into account the kinematical scattering matrix can be divided on two independent matrixes separately for waves of π-polarization and of σ-polarization because $(\mathbf{e}_m^\pi \mathbf{e}_{m'}^\sigma) = 0$ for any m, m' . However, for making a computer calculation it is not necessary to take this into account in explicit form. The separation will occur automatically.

Let the incident plane wave for the first block have the amplitude $B_{is}^{(1)}$ (normalized along the surface of the crystal), and the wave vector $\mathbf{K}_i$, namely,

$$\mathbf{E}_i^{(1)} = \gamma_{i1}^{-1/2} B_{is}^{(1)} \mathbf{e}_i^s \exp(i\mathbf{K}_i \mathbf{r}).$$

The unit vector normal to the surface is denoted $\mathbf{n}_1$ and we use a general notation $\gamma_{mk} = (\mathbf{s}_m \mathbf{n}_k)$. Here $\mathbf{K}_i = K_b \mathbf{s}_i + \mathbf{q}_i$ where $\mathbf{s}_i$ is the unit vector of direction which satisfies the multiple geometrical Bragg conditions while $\mathbf{q}_i$ is a vector of small deviation of the incident wave vector from the reference wave vector both angular and in magnitude

$$(K_b \mathbf{s}_i + \mathbf{h}_m - \mathbf{h}_i)^2 = K_b^2, \quad \mathbf{q}_i = K_b(\Delta\theta_{1i} \mathbf{e}_i^\pi + \Delta\theta_{2i} \mathbf{e}_i^\sigma + \Delta\theta_\omega \mathbf{s}_i). \tag{3}$$

The diffracted along $\mathbf{s}_j$ plane wave in air will be

$$\mathbf{E}_j^{(2)} = \gamma_{j1}^{-1/2} B_{js}^{(2)} \mathbf{e}_j^s \exp(i\mathbf{K}_j \mathbf{r}), \qquad B_{js}^{(2)} = M_{ji}^{ss(1)}(\mathbf{q}_i)\, B_{is}^{(1)}, \tag{4}$$

Here $M_{ji}^{ss(1)}(\mathbf{q}_i)$ is the element of the dynamical scattering matrix in which the polarization index is shown in explicit form. The index (1) shows that the diffraction takes place in the first block having the internal normal to the entrance surface $\mathbf{n}_1$.

The wave vector of outgoing plane wave is

$$\mathbf{K}_j = K_b \mathbf{s}_j + \mathbf{q}_j, \qquad \mathbf{q}_j = \mathbf{q}_i - \frac{K_b}{2\gamma_{j1}} \alpha_j(\mathbf{q}_i)\, \mathbf{n}_1 \tag{5}$$

The correspondence between $\mathbf{q}_j$ and $\mathbf{q}_i$ has been explained previously (see the solution of the task in one crystal plate in topic I.). When this wave falls on the second block it excites the same set of diffracted waves, but under condition of another surface orientation. Let the internal normal to the second surface be $\mathbf{n}_2$ and we are interested in outgoing plane wave along the direction $\mathbf{s}_k$. Then the necessary formulas can be written similarly to the preceding case, namely, $\mathbf{E}_k^{(3)} = \gamma_{k2}^{-1/2} B_{ks}^{(3)} \mathbf{e}_k^s \exp(i\mathbf{K}_k \mathbf{r})$ with the amplitude and the wave vector which are defined as follows

$$B_{ks}^{(3)} = M_{kj}^{ss(2)}(\mathbf{q}_j)\, B_{js}^{(2)}, \quad \mathbf{K}_k = K_b \mathbf{s}_k + \mathbf{q}_k, \quad \mathbf{q}_k = \mathbf{q}_j - \frac{K_b}{2\gamma_{k2}} \alpha_k(\mathbf{q}_j)\, \mathbf{n}_2 \tag{6}$$

We note that in calculating the second reflection the three-beam diffraction task is solved under condition that the wave along $\mathbf{s}_j$ is the incident wave while the wave along $\mathbf{s}_i$ is the diffracted wave. However, we may use the same order of reciprocal lattice vectors that leads to the same matrix of kinematical scattering amplitude $g^{ss'}_{mm'}$ of Eq.(46) in topic I. However the total kinematical scattering matrix $G^{ss'}_{mm'}(\mathbf{q}_j)$ becomes different because it contains $\alpha_m(\mathbf{q}_j)$ instead of $\alpha_m(\mathbf{q}_i)$ and γ_{m2} instead of γ_{m1}.

The third block of the monochromator, for example, may scatter the wave along $\mathbf{s}_k$ to the wave along $\mathbf{s}_i$, namely, $\mathbf{E}'_i = \gamma_{i3}^{-1/2} B'_{is} \mathbf{e}^s_i \exp(i\mathbf{K}'_i\mathbf{r})$ which will be approximately parallel to the initial wave and will have the same polarization. However the amplitude of "monochromatized" wave will be

$$B'_{is} = M^{ss(3)}_{ik}(\mathbf{q}_k) M^{ss(2)}_{kj}(\mathbf{q}_j) M^{ss(1)}_{ji}(\mathbf{q}_i) B_{is} \tag{7}$$

while the wave vector

$$\mathbf{K}'_i = K_b \mathbf{s}_i + \mathbf{q}'_i, \qquad \mathbf{q}'_i = \mathbf{q}_k - \frac{K_b}{2\gamma_{i3}} \alpha_i(\mathbf{q}_k)\, \mathbf{n}_3 \tag{8}$$

One may introduce the "transmissivity" of the monochromator as $P^s_{00} = B'_{0s}/B_{0s}$. The transmissivity is a function of angular and frequency deviations of initial beam or the same characteristics of the transmitted wave through the definition $\mathbf{q}'_i = K_b(\Delta\theta'_{1i}\mathbf{e}^\pi_i + \Delta\theta'_2\mathbf{e}^\sigma_i + \Delta\theta_\omega \mathbf{s}_i)$ and because the $\mathbf{q}'_i$ vector is connected with $\mathbf{q}_i$ vector. Despite the fact that the analytical formulas may be rather cumbersome the computer calculation of general case of geometry along the drawn above scheme is rather simple.

We note that the connection between the incoming deviation vector $\mathbf{q}_i$ and the outgoing deviation vector $\mathbf{q}_j$ in each reflection may be expressed in terms of the transition matrix $\widehat{T}_{ji}$ which describes the connection as a product of the matrix and the vector

$$\begin{pmatrix} \Delta\theta_{1j} \\ \Delta\theta_{2j} \\ \Delta\theta_\omega \end{pmatrix} = \widehat{T}_{ji} \cdot \begin{pmatrix} \Delta\theta_{1i} \\ \Delta\theta_{2i} \\ \Delta\theta_\omega \end{pmatrix} \tag{9}$$

In general case the explicit form of the transition matrix follows from Eqs.(59), (60) of topic I and may be written as follows

$$\widehat{T}_{ji} = \begin{pmatrix} \frac{(\mathbf{n}[\mathbf{e}^\pi_i \times \mathbf{e}^\sigma_j])}{(\mathbf{n}\mathbf{s}_j)} & \frac{(\mathbf{n}[\mathbf{e}^\sigma_i \times \mathbf{e}^\sigma_j])}{(\mathbf{n}\mathbf{s}_j)} & \frac{(\mathbf{n}\mathbf{e}^\pi_j)+(\mathbf{n}[\mathbf{s}_i \times \mathbf{e}^\sigma_j])}{(\mathbf{n}\mathbf{s}_j)} \\ \frac{(\mathbf{n}[\mathbf{e}^\pi_j \times \mathbf{e}^\pi_i])}{(\mathbf{n}\mathbf{s}_j)} & \frac{(\mathbf{n}[\mathbf{e}^\pi_j \times \mathbf{e}^\sigma_i])}{(\mathbf{n}\mathbf{s}_j)} & \frac{(\mathbf{n}\mathbf{e}^\sigma_j)+(\mathbf{n}[\mathbf{e}^\pi_j \times \mathbf{s}_i])}{(\mathbf{n}\mathbf{s}_j)} \\ 0 & 0 & 1 \end{pmatrix}. \tag{10}$$

The usage of transition matrixes allows us to describe the parameter of deviation from the Bragg condition for each reflection in terms of incident deviation vector and to draw the Du Mond diagram for each particular case. In case of coplanar diffraction when the normal to the surface lies in the scattering plane we may simplify further the matrix

$$\widehat{T}_{ji} = \begin{pmatrix} 1 & 0 & 0 \\ 0 & \frac{(\mathbf{n}\mathbf{s}_i)}{(\mathbf{n}\mathbf{s}_j)} & \frac{(\mathbf{n}\mathbf{e}^\sigma_j)-(\mathbf{n}\mathbf{e}^\sigma_i)}{(\mathbf{n}\mathbf{s}_j)} \\ 0 & 0 & 1 \end{pmatrix} \tag{11}$$

The method described above may be used in case of more reflections. Since the two-beam diffraction is a particular case of many-beam diffraction these formulas are valid for two-beam monochromator as well. However in case of two-beam diffraction one has a possibility to develop further the analytical analysis. In case of many-beam diffraction the complete solution of the problem is based on the computer calculations. The basic features of the formulation presented above was developed in article

- V. G. Kohn, Phys. Status Solidi (a), 1979, vol. 54, p. 375

Below we shall consider in detail several particular cases.

3. COPLANAR MULTIPLE DIFFRACTION. SPECIFIC EXAMPLES.

3.1 Graeff-Bonse interferometer

In 1977 Graeff and Bonse have proposed the new type of interferometer in the paper

- W. Graeff, U. Bonse, Z. Phys. B, 1977, vol. 27, p. 19

The interferometer uses the coplanar (440), (044) three-beam diffraction in Silicon for a wavelength of the radiation $\lambda_c = 1.663$ Å which is close to Ni K_α fluorescent radiation. Fig.2 (left) shows the direction of different beams together with the index m of the beams and the vectors $\mathbf{s}_m$ and $\mathbf{e}_m^\sigma$ in this case. The interferometer has five blocks which are the different parts of the same crystal. The arrangement of blocks and the path of the interfering beams are shown in Fig.2 (right). The first block divides the incident beam number 1 on two beams simultaneously owing to two reflections on the atomic planes which corresponds to the reciprocal lattice vectors (440) and (044). These beams have

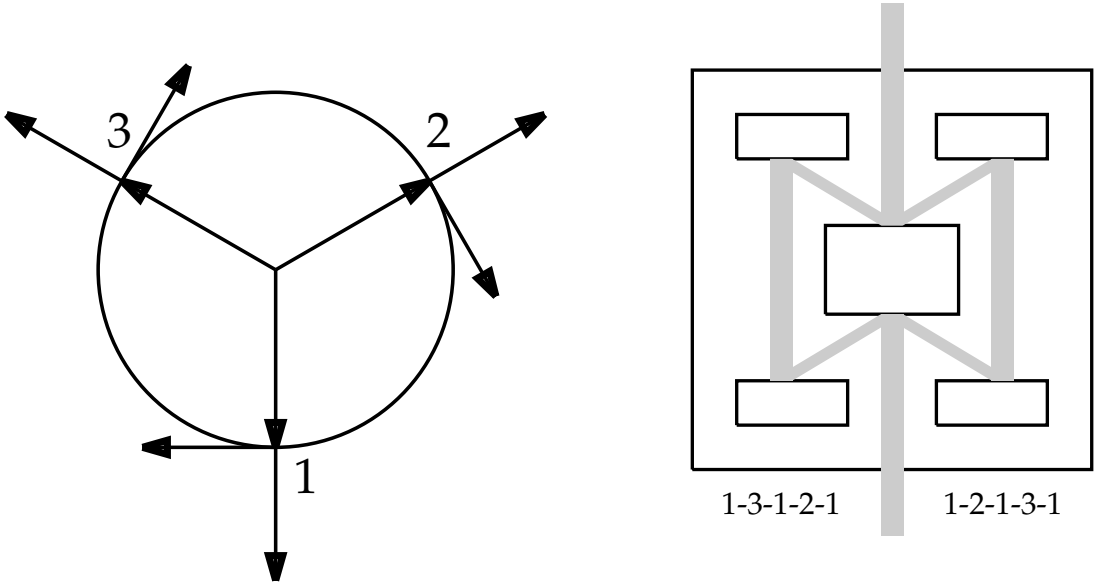

FIG. 2. Directions and polarizations of the waves in coplanar (400),(044) three-beam diffraction (left) and the ray trajectories in the Graeff-Bonse interferometer (right)

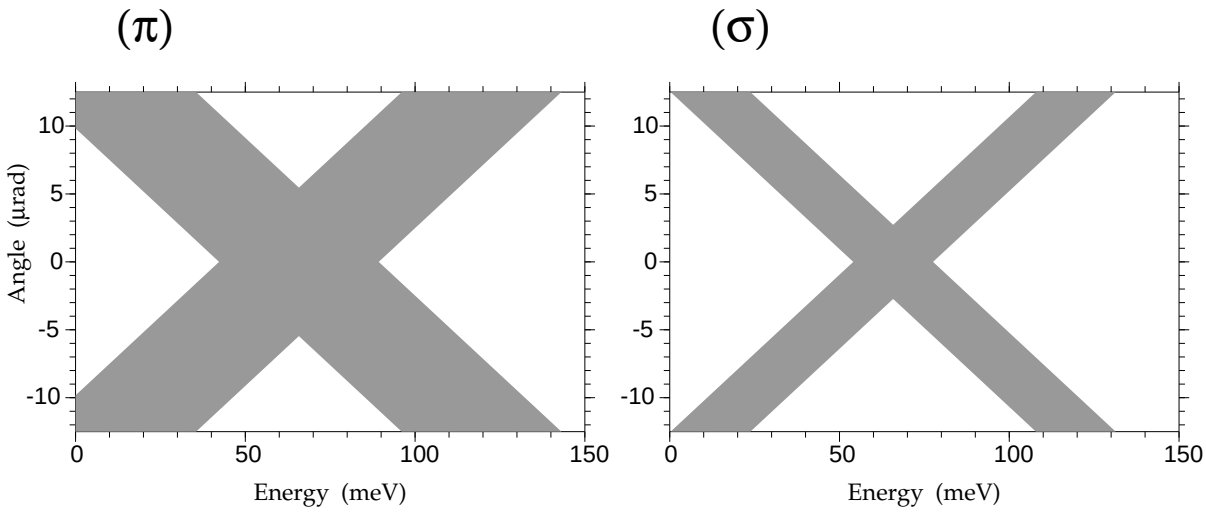

FIG. 3. Two-beam transmissivity map for Graeff-Bonse interferometer similar to Du Mond diagram

indexes 2 and 3. Then both the right and the left beam go on symmetrical trajectories where only one reflection is used among the two possible reflections. Finally the beams meet each other on the opposite side of the first block and after fourth reflection the wave field becomes a superposition of the wave fields of two beams. The right part corresponds to the chain 1-2-1-3-1 while the left part corresponds to the chain 1-3-1-2-1. If the interfering waves have different phases in space across the beams then the resulting intensity will show the oscillating behavior which is usually called interference fringes.

The advantage of such the devices is that the necessity to adjust the different blocks is absent. The usage of the Bragg geometry promises, generally speaking, the high reflectivity because the decrease of the intensity due to an absorption is minimal. In addition, the thick blocks can be used which is convenient from the technological point of view. However, this arrangement has the disadvantage just owing to the same reasons. First of all, it is the well known property of the diffraction in the Bragg geometry that the real angular region of the reflectivity maximum is shifted from the region followed from the kinematical Bragg condition. In other words, the maximum of reflectivity occurs at finite values of the parameters $\Delta\theta_2$, $\Delta\theta_\omega$ which may be different in different reflections. The same crystal lattice can provide the automatic fulfillment of the kinematical Bragg condition only. Therefore one needs in good luck to satisfy the dynamical Bragg condition simultaneously in all blocks because one has no the possibility to fine adjust the different blocks as in the case of separate crystals.

It is clear now that we have no the instrument for changing the transmissivity of such the device. We can only calculate how much transmissivity we may obtain for such an arrangement using the multiple diffraction theory described above. There may be different levels of accuracy of such a calculation. The simplest estimation of transmissivity is obtained when one takes into account the two-beam regions of reflectivity maximum of each crystal. Let us consider the transition from i-th beam to j-th beam with $\gamma_i > 0$ and

$\gamma_j < 0$. For each polarization state we can separate two equations from the whole set of equations $\varepsilon B_m = \sum_{m'} G_{mm'} B_{m'}$ obtained in the topic I, namely,.

$$\begin{aligned} \varepsilon B_i &= G_{ii} B_i + G_{ij} B_j \\ \varepsilon B_j &= G_{ji} B_i + G_{jj} B_j \end{aligned} \tag{12}$$

and the region of reflectivity maximum is described by the equation

$$(G_{ii} - G_{jj})^2 + 4 G_{ij} G_{ji} < 0 \tag{13}$$

A substitution of the explicit form of the matrix elements

$$G_{mm'} = \frac{K}{(\gamma_m \gamma_{m'})^{1/2}} [-\alpha_m \delta_{mm'} + g_{mm'}] \tag{14}$$

obtained in topic I to this condition leads to the next formula for the value of parameter $\alpha_j(i)$ which describes the deviation from the Bragg condition with i-th beam as an incident one and j-th beam as a reflected one at the boundaries of the reflectivity maximum

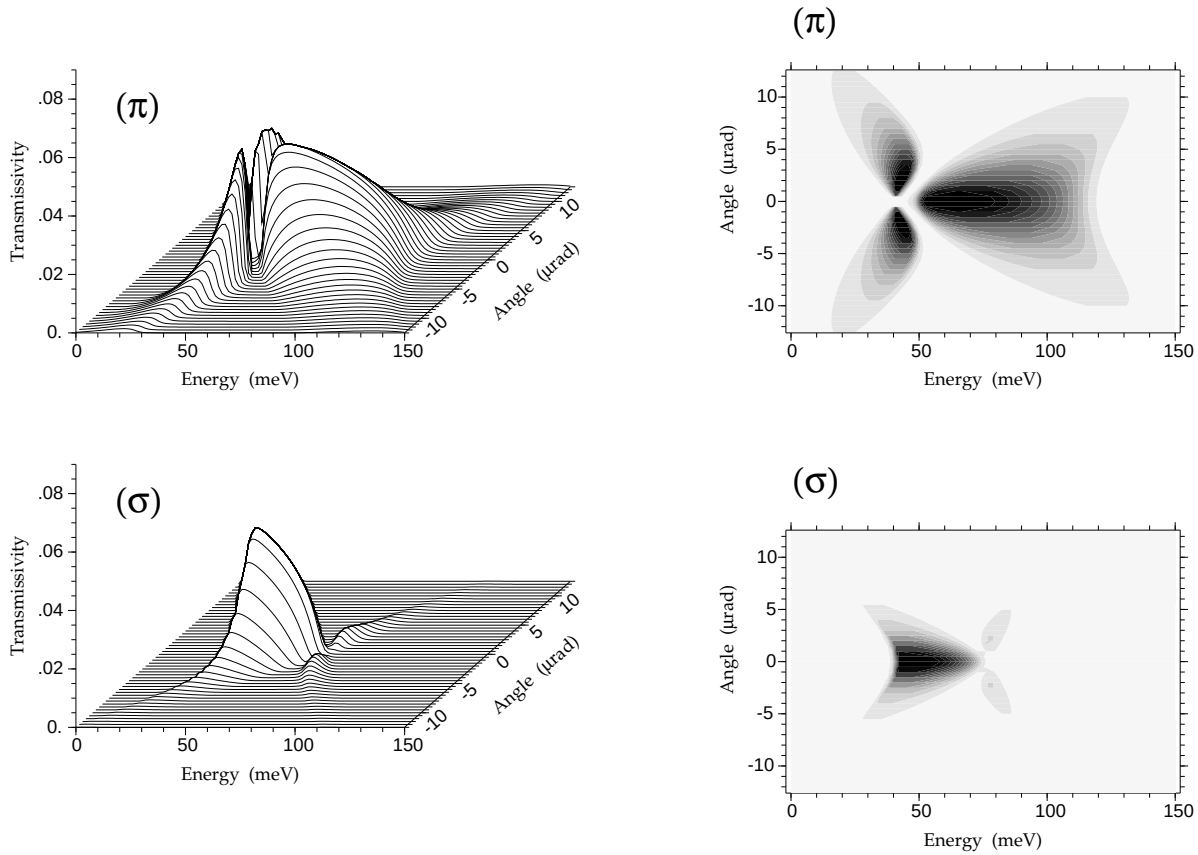

FIG. 4. The transmissivity of the Graeff-Bonse interferometer in the energy - angle coortinate plane, 3D-sight (left) and the same as a map of levels (right). The black marks the region with $f > 0.035$

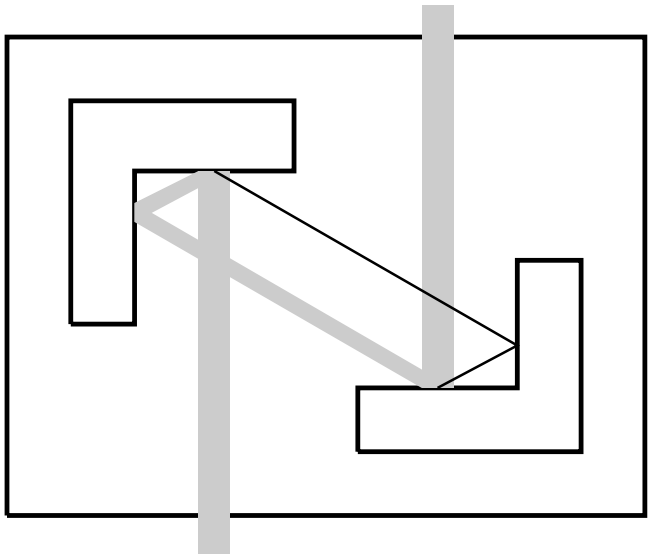

FIG. 5. The ray trajectories in the Gabrielyan-Kohn monochromator

$$\alpha_j(i)_{\rm limit} = -\chi_0\left(1+\frac{|\gamma_j|}{\gamma_i}\right) \pm 2\,(\mathbf{e}_i\mathbf{e}_j)\sqrt{\frac{|\gamma_j|}{\gamma_i}}\sqrt{\chi_h\chi_{\overline{h}}} = A^{(a)}_{ji}\Delta\theta_{2i} + A^{(e)}_{ji}\Delta\theta_\omega \qquad (15)$$

On the other hand, the angle $\Delta\theta_{2i}$ can be expressed in terms of angular deviation of the incident beam for the first block (incoming beam) using the transition matrix of Eq.(11).

The result of such an estimation is shown on Fig.3 for π and σ polarization states separately. The width of strips in case of σ-polarization is less than one of π-polarization owing to non-unity polarization factor $(\mathbf{e}_i\mathbf{e}_j)$. The map of such a type is similar to the well known Du Mond diagram of the theory of two-beam monochromators. However, in case of three-beam diffraction in each block the reflectivity maximum may have different shape and, in addition, the total reflection may be absent because the part of the intensity is brought by second reflecting beam. Therefore the accurate three-beam calculation is necessary to obtain the real transmissivity distribution. The results of such a calculation in case of the Graeff-Bonse interferometer is shown in Fig.4 (left) as a quasi 3D picture for π and σ polarizations separately. As shown at the figure the reflectivity is not complete in each reflection. As a result, the maximum value of transmissivity is not high - only about three per cent. The angular and energy dependences becomes rather complicated. The calculation presented here was fulfilled by author of these notes and it takes into account the absorption of X-rays. In the original article of Graeff and Bonse (see above a citation) have presented the results of calculation when the absorption was neglected. In this case the maximum value was six per cent that is twice larger. The comparison shows that the absorption cannot be neglected.

On the other hand, the region of the transmissivity maximum is symmetrical in terms of $\Delta\theta_2$ axis. It is necessary condition for observing the interference fringes that the both shoulders of the interferometer would have the same region of transmissivity maximum.

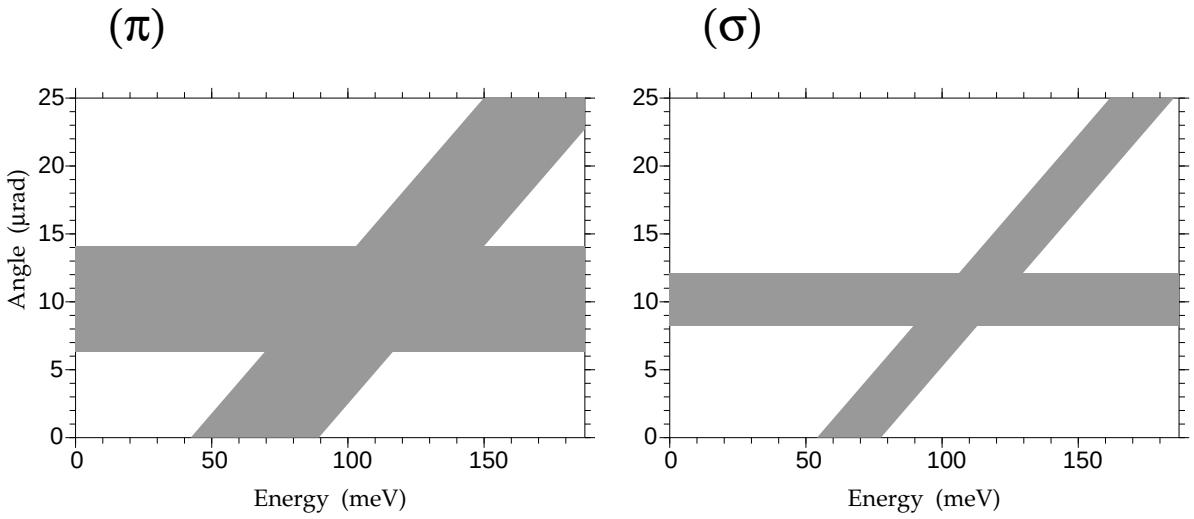

FIG. 6. Two-beam transmissivity map for Gabrielyan-Kohn monochromator similar to Du Mond diagram

The form of presentation of Fig.4 (left) is not convenient to analyze this property. This is why the Fig.4 (right) shows the same distribution as a map of levels. This form of presentation is good enough to analyze the position of singular points.

3.2 Three-wave monochromator

As was pointed out above we need in the intersection of dynamical regions of reflectivity maximums for each crystal block of the device to obtain the maximum transmissivity. From this point of view the scheme having three blocks instead of four blocks, where one of the blocks has a surface perpendicular to two others may be preferential. Such a device as a monochromator was proposed in 1980 by Gabrielyan and Kohn in the paper

- R. Z. Gabrielyan, V. G. Kohn, Phys. Status Solidi, (a), 1980, vol. 59, p. 697.

The ray paths inside such a device which correspond to a channel 1-3-2-1 and 1-2-3-1 are shown in Fig.5. One can see the reflection 3-2 of path 1-3-2-1 is symmetrical and in this case the beam 1 goes along the surface. For our purpose we may exclude this beam from the consideration and consider this reflection as two-beam reflection. Therefore we obtain a good two-beam reflectivity in one of reflections. In addition the region of reflectivity maximum becomes shifted from the origin on the axis of angle. This leads to larger values of reflectivity in other reflections

Just owing to a good luck in meeting the dynamical regions of reflectivity maximums this device has much more value of the transmissivity maximum. Similar to the preceding analysis the Fig.6 shows the rough estimation of the region where we may expect the maximum of the reflectivity. The Fig.7 shows the results of accurate calculation of transmissivity in this case as a three dimensional surface and as a map of levels. One can see the maximum reaches 70 per cent. However, the region of maximum corresponds to positive values of $\Delta\theta_2$ shifted from the origin and therefore it is not symmetrical. The

other ray path 1-2-3-1 would have the transmissivity maximum in the region of negative $\Delta\theta_2$. As a result, the interference fringes will appear in the initial state of the interferometer which will mask all extra phase disturbances. To exclude this effect one may use the wedge in one of the shoulder of the interferometer.

3.3 Four-wave monochromator.

From the point of view of Mössbauer effect the wavelength $\lambda = 0.860$ Å (the energy $\hbar\omega = 14.41$ keV) is of interest which corresponds to nuclear resonant radiation of ^{57}Fe nucleus. It is turned out that in Silicon crystal lattice having crystal lattice parameter $a = 5.43$ Å, the four-wave coplanar case $(440, 84\overline{8}, 0\overline{48})$ corresponds to $\lambda_c = 0.859$ Å which is just very close to the necessary wavelength. Therefore I decide to analyze this case using the same approach and software which was used in preceding consideration. This result is new and it is not published elsewhere. The Fig.8 shows the direction of rays and polarization vectors in this case. One can see that the rays with numbers 2 and 3 as well as the rays with numbers 1 and 4 have the angle of the 90°. Therefore no one ray cannot be

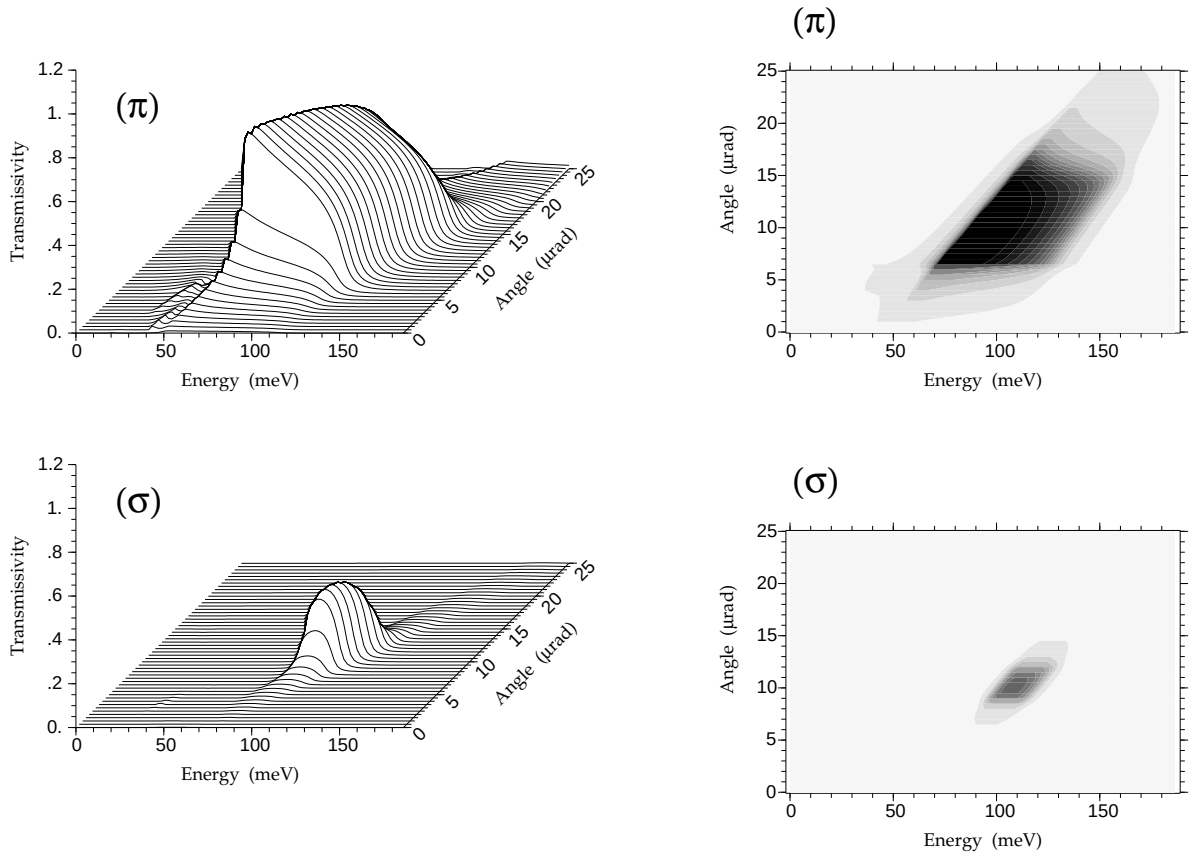

FIG. 7. The transmissivity of the Garielyan-Kohn monochromator in the energy - angle coortinate plane, 3D-sight (left) and the same as a map of levels (right). The black marks the region with $f > 0.6$

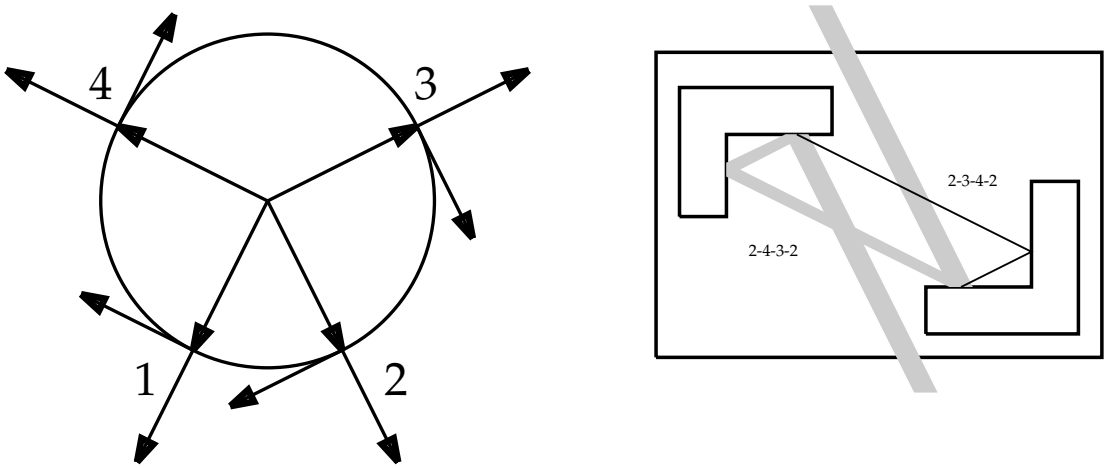

FIG. 8. Directions and polarizations of the waves in the coplanar (400),(84$\overline{8}$),(0$\overline{48}$ four-beam diffraction (left) and the ray trajectories in the four-beam monochromator (right)

normal to the entrance surface of the crystal. The scheme of the possible monochromator may be as shown in Fig.9 which uses the 2-4-3-2 ray path. The Fig.10 shows the two-beam regions of reflectivity maximum as it was explained in analysis the Graeff-Bonse interferometer. Contrary to preceding cases here each crystal has independent region and the match of these regions exists only approximately. In addition the map for σ-polarized radiation has zero thickness line for 3-2 transition because the polarizations of these rays cannot interact with each other.

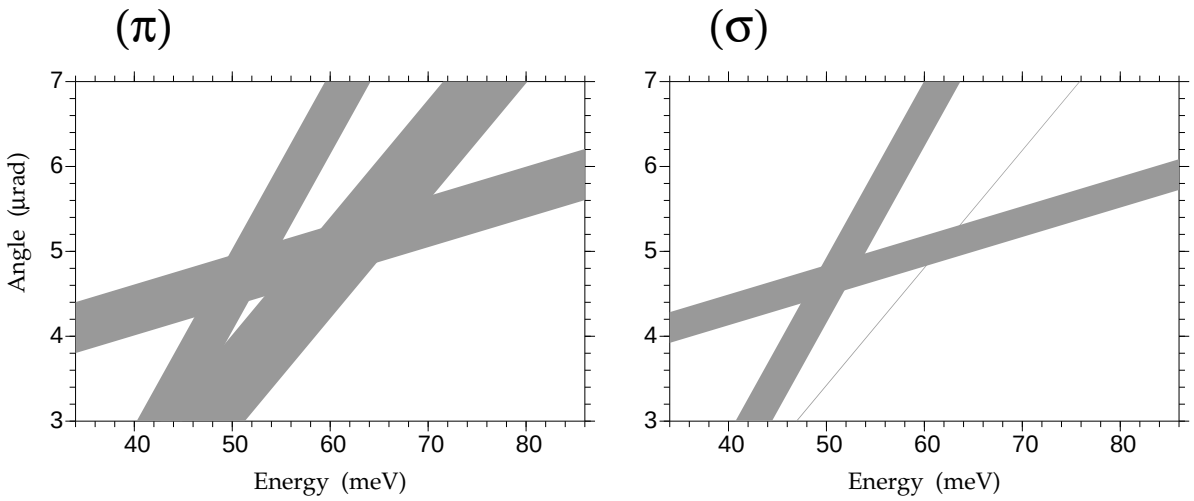

FIG. 9. Two-beam transmissivity map for the four-beam monochromator similar to Du Mond diagram

Bearing in mind such an information it is difficult to expect rather high value of transmissivity of this device. However, the accurate calculation shown in Fig.10 (left) allows to conclude that at least π-polarized radiation can reach six per cent transmissivity that is larger than in case of Graeff-Bonse interferometer. The structure of the maximum is unusual and consists of two separate regions. One of them is thick enough while another is thin. The Fig.10 (right) shows the same distribution as a map of levels where this property is seen rather well. It is of interest to note that the σ-polarized radiation also has a finite trasmissivity. The reason of this fact is one of the property of multiple diffraction to excite the forbidden two-beam reflections through the interaction with other rays. This effect is not small when the conditions of dynamical diffraction becomes fulfilled.

As it was pointed out above in using the monocrystal monochromator having several blocks one has no a possibility to perform a fine adjustment of angular position of the blocks to match the dynamical Bragg conditions in all the blocks simultaneously. However, the proper choice of the orientation of the entrance surface of the blocks can solve this problem in reasonable limits. It is seen clearly from the comparison of the two different three-beam devices considered above. Probably, it is possible to make an optimization the four-beam monochromator in such a way. This work is not made up to now.

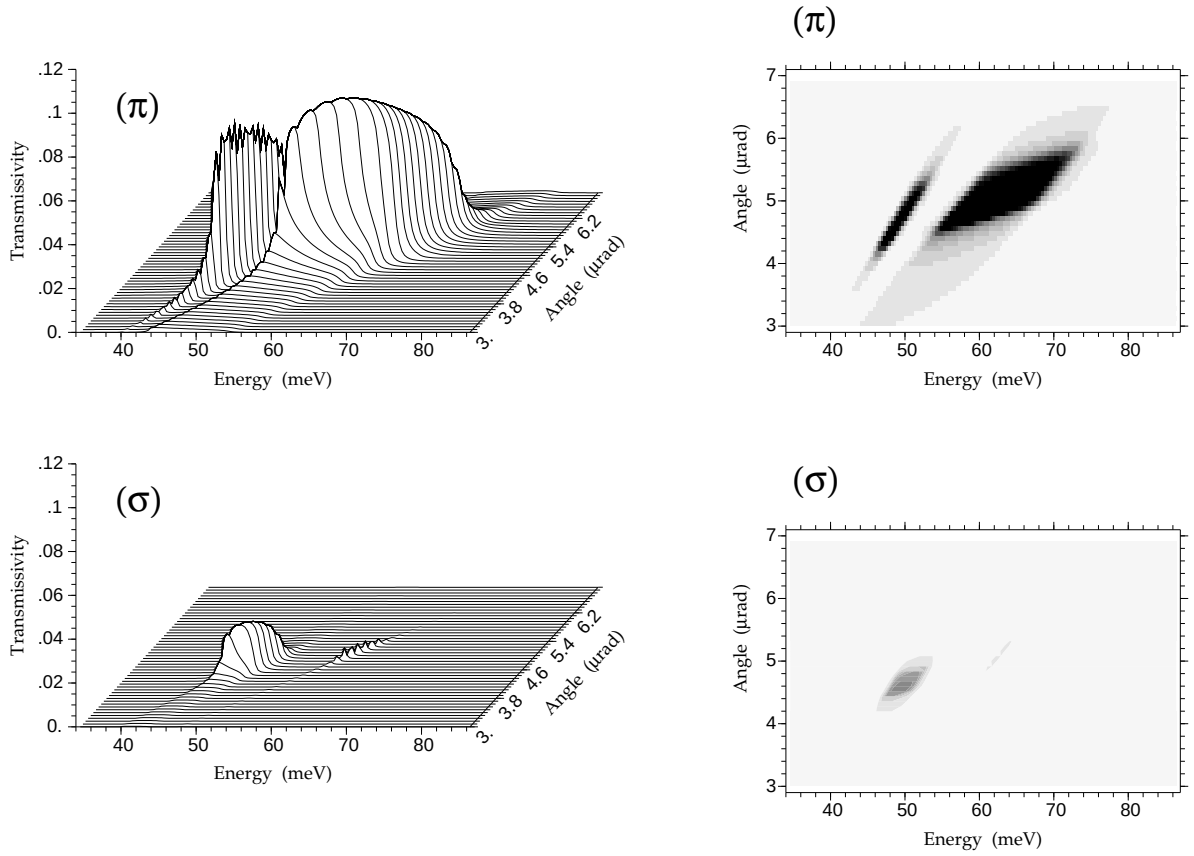

FIG. 10. The transmissivity of the four-beam monochromator in the energy - angle coortinate plane, 3D-sight (left) and the same as a map of levels (right). The black marks the region with $f > 0.05$

4. THE THEORY OF MULTIPLE DIFFRACTION IN MULTILAYER CRYSTAL SYSTEM

The multilayer crystal system presents by itself the another relatively simple system where the all crystal plates (layers) have the surfaces which is parallel to each other. These surfaces can be represented by the unit vector of internal normal **n**. The atomic composition of each layer will be different as well as crystal lattice parameters. We will assume only that some of the layers have almost the same crystal lattice parameters, so that the multiple diffraction is realized on the same reciprocal lattice vectors. Practically such a system may be managed by heteroepitaxial growth of the different layers on a substrate under different conditions.

The problem of calculating the parameters of multiple diffraction in such a system naturally is divided on two stages. At the first stage we may calculate the unknown waves outgoing from each layer from the incoming waves to the layer. It is not necessary to know the incoming waves themselves because we may calculate only the dynamical scattering matrixes of each layer on the same set of reciprocal lattice vectors. How to do this is described in the topic I. However, for a complete solution of the problem we need to solve the self-consistent task because the outgoing waves from one layer become incoming waves for another layer. One of ways of solving this self-consistent problem is based on the recurrent relations. These recurrent relation are similar to the Parratt recurrent relation in the theory of grazing incidence multilayer systems (multilayer mirrors). However, in case of multiple diffraction these relations turn out to be much more complicated.

To described the method of solution we shall use the notation developed for one crystal

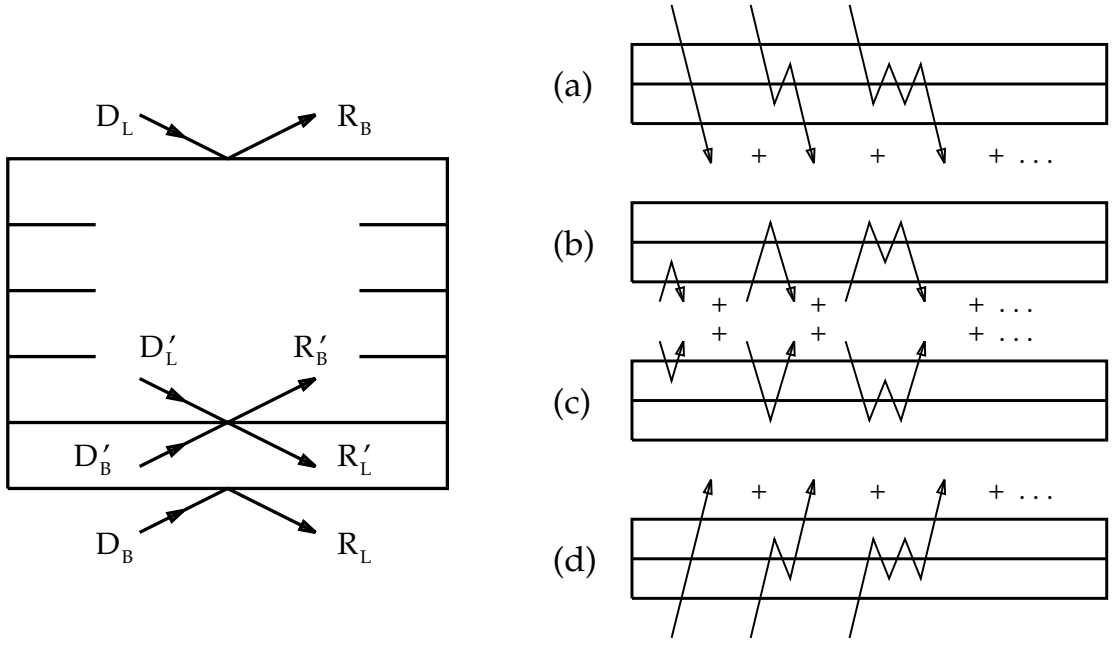

FIG. 11. The scheme showing a relation between incoming and outgoing waves at different boundaries of two-layer system (left) and the schemes showing the multiple scattering processes between layers (right)

plate, namely, the index L will denote all transmitted waves ($\gamma_m > 0$) and all eigenvalues with $\varepsilon_j'' > 0$ while the index B will denote all reflected waves ($\gamma_m < 0$) and all eigenvalues with $\varepsilon_j'' < 0$. Let us isolate the subsystem consisting of the k upper layers and the $(k+1)$-th upper layer. The $(k+1)$-th layer is described by the dynamical scattering matrix $M_{ij}^{(k+1)}$ where $i, j = L, B$. We may describe the system of k upper layers by the matrix $W_{ij}^{(k)}$. We assume that these matrixes are known. The problem is to determine the matrix $W_{ij}^{(k+1)}$ for the system of $(k+1)$ layers. The latter defines the relations between the known waves D_L, D_B and the unknown waves R_L, R_B while the matrix $M_{ij}^{(k+1)}$ defines the relations between D_L', D_B and R_L', R_B. On the other hand, the matrix $W_{ij}^{(k)}$ defines the relations between D_L, D_B' and R_L', R_B.

It is easy to understand examining the Fig.11 (left) that

$$D_L' = R_L', \qquad D_B' = R_B' \tag{16}$$

On the other hand, the known matrixes allows us to write directly the relations

$$R_L' = W_{LL}^{(k)} \cdot D_L + W_{LB}^{(k)} \cdot D_B' \tag{17}$$
$$R_B = W_{BL}^{(k)} \cdot D_L + W_{BB}^{(k)} \cdot D_B' \tag{18}$$

for k upper layers system and

$$R_L = M_{LL}^{(k+1)} \cdot D_L' + M_{LB}^{(k+1)} \cdot D_B \tag{19}$$
$$R_B' = M_{BL}^{(k+1)} \cdot D_L' + M_{BB}^{(k+1)} \cdot D_B \tag{20}$$

The our task is to find the direct relations between R_L, R_B and D_L, D_B using the above written formulas. It is a relatively simple algebraic problem. First of all, we find from the equations (17) and (20)

$$\begin{aligned} R_L' &= (I_{LL} - W_{LB}^{(k)} \cdot M_{BL}^{(k+1)})^{-1} \cdot (W_{LL}^{(k)} \cdot D_L + W_{LB}^{(k)} \cdot M_{BB}^{(k+1)} \cdot D_B) \\ R_B' &= (I_{BB} - M_{BL}^{(k+1)} \cdot W_{LB}^{(k)})^{-1} \cdot (M_{BL}^{(k+1)} \cdot W_{LL}^{(k)} \cdot D_L + M_{BB}^{(k+1)} \cdot D_B) \end{aligned} \tag{21}$$

Using these relations we find finally

$$\begin{aligned} R_L &= W_{LL}^{(k+1)} \cdot D_L + W_{LB}^{(k+1)} \cdot D_B \\ R_B &= W_{BL}^{(k+1)} \cdot D_L + W_{BB}^{(k+1)} \cdot D_B \end{aligned} \tag{22}$$

where

$$\begin{aligned} W_{LL}^{(k+1)} &= M_{LL}^{(k+1)} \cdot (I_{LL} - W_{LB}^{(k)} \cdot M_{BL}^{(k+1)})^{-1} \cdot W_{LL}^{(k)} \\ W_{LB}^{(k+1)} &= M_{LB}^{(k+1)} + M_{LL}^{(k+1)} \cdot (I_{LL} - W_{LB}^{(k)} \cdot M_{BL}^{(k+1)})^{-1} \cdot W_{LB}^{(k)} \cdot M_{BB}^{(k+1)} \\ W_{BL}^{(k+1)} &= W_{BL}^{(k)} + W_{BB}^{(k)} \cdot (I_{BB} - M_{BL}^{(k+1)} \cdot W_{LB}^{(k)})^{-1} \cdot M_{BL}^{(k+1)} \cdot W_{LL}^{(k)} \\ W_{BB}^{(k+1)} &= W_{BB}^{(k)} \cdot (I_{BB} - M_{BL}^{(k+1)} \cdot W_{LB}^{(k)})^{-1} \cdot M_{BB}^{(k+1)} \end{aligned} \tag{23}$$

Here I_{LL} and I_{BB} are identity matrixes of appropriate dimensions. The formulas (23) are the required recurrent relations. These allow us to calculate the total dynamical scattering

matrix of the system containing N layers by means of calculating the dynamical scattering matrixes of each layer and then successively applying the recurrent relation N-1 times with 1+2, (1+2)+3, ..., (1+2+...+[N-1])+N. The approach presented above was developed by author in the article

- V. G. Kohn, J. Moscow Phys. Soc., 1991, vol. 1, p. 425

The physical meaning of the formulas (23) becomes clear if we expand the multiplicative inverse matrixes in power series. This allows us to represent the formulas as the sum of processes of multiple reflection and transmission of the waves in the layers. These processes are shown schematically in Fig.11 (right) for the LL (a), BL (b), LB (c) and BB (d) scattering geometries. The method of summing the series expansion can give also the equivalent result in a somewhat different form. For instance

$$W_{BL}^{(k+1)} = W_{BL}^{(k)} + W_{BB}^{(k)} \cdot M_{BL}^{(k+1)} \cdot (I_{LL} - W_{LB}^{(k)} \cdot M_{BL}^{(k+1)})^{-1} \cdot W_{LL}^{(k)}. \tag{24}$$

If the $(k+1)$-th layer if very thick (substrate), then only this matrix is of interest and we can employ the approximation of Eq.(70) of topic I for $M_{BL}^{(k+1)}$.

To understand better the recurrent relations we may bear in mind that these must work in the two-beam diffraction case as well. In this case the matrixes are reduced to values and the next notation is usually employed $M_{LL} = t$, $M_{BL} = r$, $M_{LB} = \overline{r}$, $M_{BB} = \overline{t}$. Now the formulas (23) may be written as

$$T_{k+1} = \frac{t_{k+1} T_k}{1 - r_{k+1}\overline{R}_k}, \qquad \overline{T}_{k+1} = \frac{\overline{t}_{k+1}\overline{T}_k}{1 - r_{k+1}\overline{R}_k},$$

$$R_{k+1} = R_k + \frac{r_{k+1} T_k \overline{T}_k}{1 - r_{k+1}\overline{R}_k}, \qquad \overline{R}_{k+1} = \overline{r}_k + \frac{\overline{R}_k t_{k+1}\overline{t}_{k+1}}{1 - r_{k+1}\overline{R}_k}. \tag{25}$$

In the problem of epitaxial layered system on a thick substrate or in the case of grazing incidence multilayer mirror or in case of crystal under the condition of temperature gradient near the surface it is convenient to use the recurrent relations from bottom to top of the system and only the reflectivity is of interest. The corresponding formula for the two-beam diffraction case may be obtained from the above written formula by simple replacement r_{k+1} by R_k and so on. As a result, we obtain the formula which connects the reflectivity of system of $(k+1)$ layers with the reflectivity of system of k layers which depends only on the parameters of $(k+1)$-th layer as follows

$$R_{k+1} = r_{k+1} + \frac{t_{k+1}\overline{t}_{k+1} R_k}{1 - \overline{r}_{k+1} R_k} \tag{26}$$

The formula of such a type can be obtained in case of multiple diffraction by replacement of r by M_{BL}, R by W_{BL} and so on. The interesting particular case of multilayer system is a multilayer superlattice when one can select the layers with the same properties which repeat themselves periodically. In this case the parameters of layer does not depend on the index of layer and the recurrent relation has the more simple form

$$R_{k+1} = r + \frac{t\overline{t} R_k}{1 - \overline{r} R_k}. \tag{27}$$

It is of interest that this relation has an analytical solution as was shown by author in the article

- V. G. Kohn, Phys. Status Solidi (b), 1995, vol. 187, p. 61.

This analytical solution is expressed through the Chebyshev's polynomials and may be written in the form closed to the expression of reflectivity amplitude of two-beam dynamical diffraction with generalized scattering amplitudes instead of χ_0, χ_h.

5. POSSIBLE INTERESTING PHENOMENA

The formulas obtained above allow to solve many different problems of multiple dynamical scattering and to consider different multilayer systems. One of the interesting phenomenon arises in two-layer system under the three beam diffraction. It occurs when one Bragg condition is satisfied well while another Bragg condition is satisfied only approximately. Then we obtain the situation when one of two reflected beams is strong while the second beam has a small amplitude. It is clear that the weak reflection cannot influence the interaction of the strong waves. On the other hand, the angular dependence of intensity of this weak reflection is sensitive to the both strong waves and the interaction is coherent. As a result, the intensity of weak reflection feels the phase shift between the strong reflected wave and the incident wave. In a single layer system we only may measure the standard phase of reflected amplitude which is predicted by dynamical theory and is described by the formulas obtained at the end of topic I. In the two-layer system an additional possibility arises. If the parameters of the upper layer is different from these of substrate we may found that the weak reflection can reveal this change of parameters through the additional phase shift.

The situation is very similar to the X-Ray Standing Wave method. The idea of such a method was formulated in the article

- V. G. Kohn, Phys. Status Solidi (a), 1988, vol.106, p.31

and then developed further in

- V. G. Kohn, L. V. Samoilova, Phys. Status Solidi (a), 1992, vol.133, p.9
- M. Kovalchuk, A. Kazimirov, V. Kohn, A. Kreines, L. Samoilova,
  . Physica B, 1996, vol.221, p.445.

Another interesting effect of multiple diffraction with strong and weak waves arises in the fine structure of Reninger's peak of forbidden reflection which can be excited by other strong reflection. Just if the second reflection is not strong but sufficient so the parameter of the deviation from the Bragg condition α_g is large but in reasonable degree only the second order scattering process is sufficient for the first forbidden reflection which has a small parameter of deviation from the Bragg condition simultaneously with zero the first order scattering amplitude $\chi_{h0} = 0$. However, the second order contribution to the scattering amplitude is sufficient now and it can be written as

$$\widetilde{\chi}_{h0} = \frac{\chi_{hg}\chi_{g0}}{\alpha_g}$$

In the Bragg case we may obtain even the total reflection (100 per cent) in the nonabsorbing crystal. In addition, the width of the reflectivity maximum will depend on the Bragg

condition for the second weak reflection and may be changed by a simple rotation of the crystal. The idea and the theoretical analysis of this case was proposed in the paper

- V. G. Kohn, Kristallografiya, 1988, vol. 33, p.567. (in Russian)

The multilayer system presents additional possibilities.

For my opinion one of the most exciting phenomenon of multiple diffraction is connected with the well known anomalous transmission effect which was discovered first experimentally by Borrmann

- G. Borrmann, Phys. Zschr., 1941, vol. 42, p. 157.

and only later it was explained theoretically. The explanation is very simple. In the two-beam diffraction the Bloch wave is the pure sine wave (X-Ray standing wave of most simple form). Under certain conditions the zero minimums of intensity of such a wave coincide with the nodes of crystal lattice. Therefore the interaction between electrons of K-shell of atoms of lattice may arise only when atoms move their positions from the lattice node due to thermal vibrations.

The multiple diffraction allows to find the condition when the intensity of X-Ray standing wave is modulated in two directions. In the six-beam case it is possible to achieve such the structure of the spatial region of intensity minimum near the lattice node when even thermal vibrations cannot excite the the photoelectron emission. The absorption becomes extremely small and it is limited only by Compton scattering or crystal lattice defects. This effect, on the contrary, was first discovered theoretically in the article

- T. Joko, A. Fukuhara, J. Phys. Soc. Japan, 1967, vol. 22, p. 597

and was analysed in detail in the works

- A. M. Afanasev, V. G. Kohn, Acta Crystall., 1977, vol. A33, p. 178
- V. G. Kohn, Fiz. Tverd. Tela, 1976, vol.18, p.2538 (in Russian)

Today there is only one accurate experimental measurement of this effect with a use of synchrotron radiation. Result is published in

- A. Yu. Kazimirov, M. V. Kovalchuk, V. G. Kohn, T. Ishikawa, S. Kikuta,
  . K. Hirano, Europhys. Lett., 1993, vol.24, p.211.

This effect is very sensitive to the angular deviations of the incident beam in two independent planes therefore for the collimation of the incident beam it is necessary to use the same six-beam phenomenon.

The more detailed discussion of these questions may be will be presented in a separate topic. However, I have no time to make this now.